

Presented at IC Channeling 2018

September 27, 2018

Published on ArXiv

October 15, 2018

Accepted by JHEP

March 12, 2019

Published on JHEP

March 26, 2019

Feasibility of τ -lepton electromagnetic dipole moments measurement using bent crystal at the LHC

A.S. Fomin,^{1,2,*} A.Yu. Korchin,^{1,3,†} A. Stocchi,^{4,‡} S. Barsuk,⁴ and P. Robbe⁴

¹*NSC Kharkiv Institute of Physics and Technology,
1 Akademicheskaya St., Kharkiv, 61108 Ukraine*

²*currently at CERN, European Organization for Nuclear Research, Geneva 23, CH-1211 Switzerland*

³*V.N. Karazin Kharkiv National University, 4 Svobody Sq., Kharkiv, 61022 Ukraine*

⁴*LAL (Laboratoire de l'Accélérateur Linéaire),
Université Paris-Sud/IN2P3, Btiment 200 — BP 34,
Rue André Ampère, 91898 Orsay Cedex, France*

In this paper we discuss the possibility of measuring the anomalous magnetic and electric dipole moments of the τ lepton. The method consists in studying the spin precession induced by the strong effective magnetic field inside channels of a bent crystal with a dedicated setup at the CERN Large Hadron Collider.

PACS number: 13.20.-v, 13.35.Dx, 13.40.Em, 13.88+e, 14.60.Fg, 61.85.+p

Keywords: Fixed target experiments, Polarisation, Tau Physics

ArXiv ePrint: [1810.06699](https://arxiv.org/abs/1810.06699)

Cite this article as:

A.S. Fomin, A.Yu. Korchin, A. Stocchi, et al. J. High Energ. Phys. 03 (2019) 156.

[arXiv:1810.06699] [https://doi.org/10.1007/JHEP03\(2019\)156](https://doi.org/10.1007/JHEP03(2019)156)

* alex.fomin@cern.ch

† korchin@kipt.kharkov.ua

‡ stocchi@lal.in2p3.fr

CONTENTS

| | |
|--|----|
| I. Introduction | 2 |
| II. Principle of the measurement | 6 |
| A. Initial polarisation of τ leptons from D_s decays | 6 |
| B. Final polarisation and energy of reconstructed τ leptons | 9 |
| C. Experimental setup | 11 |
| III. Sensitivity studies | 13 |
| A. First crystal: spectrum of deflected D_s mesons | 14 |
| B. Second crystal: spectrum and polarisation of deflected τ leptons | 16 |
| C. Preliminary study of the background from other decay channels | 19 |
| D. Results of the sensitivity studies | 20 |
| IV. Conclusions | 22 |
| A. Polarisation of τ leptons in D_s decays | 23 |
| B. Optimal length for D_s conversion to τ leptons | 24 |
| Acknowledgments | 26 |
| References | 26 |

I. INTRODUCTION

The magnetic dipole moment (MDM) of many particles has been measured [1]. For example, the experimental value of the electron MDM perfectly agrees with theoretical calculations. For muon, there is a discrepancy between the Standard Model (SM) prediction [1] (ch. 57) and measurement by the BNL E821 collaboration [2]. The deviation is about 3.5σ and it can possibly originate from effects of new physics (NP). This aspect of the muon MDM attracts considerable attention (see, *e.g.*, [3–5]).

The MDM of the τ lepton has not been measured so far and is of great interest for a test of the SM and the search for signatures of NP.

Usually one discusses the anomalous part of the MDM,

$$a_\tau = (g_\tau - 2)/2, \quad (1)$$

which is expressed through the gyromagnetic factor g_τ (or g -factor). The value $g_\tau = 2$ corresponds to a point-like Dirac particle ignoring radiative corrections. Deviations from $g_\tau = 2$ arise from the known radiative corrections and can also stem from effects of NP. The latter are of the order of m_τ^2/Λ^2 , where m_τ is the mass of τ lepton and Λ is the scale of NP. Because of the large mass of the τ lepton the effects of NP are expected to be more noticeable than the corresponding effects for muon.

The SM expectation for the τ MDM is given in Ref. [6],

$$a_{\tau, \text{SM}} = 0.00117721(5). \quad (2)$$

No measurement of the τ MDM has been performed because of the very short lifetime of the τ lepton, $2.903(5) \times 10^{-13}$ s. This does not permit to apply methods used in the electron and muon $g-2$ experiments. At present the τ anomalous magnetic moment a_τ is known to an accuracy of only about 10^{-2} [1]. This limit was obtained by the DELPHI collaboration [7] from the measurement of the $e^+e^- \rightarrow e^+e^-\tau^+\tau^-$ total cross section at LEP2. The study of anomalous couplings of photon to τ lepton in this reaction at LEP was proposed in [8]. At 95% confidence level, the confidence interval is [1]

$$-0.052 < a_\tau < 0.013. \quad (3)$$

It is also given in Ref. [7] in the form $a_\tau = -0.018(17)$. The authors of Ref. [9] analyzed LEP1, SLD and LEP2 experiments on the τ -lepton production and obtained 2σ bounds

$$-0.007 < a_\tau < 0.005. \quad (4)$$

Note that Ref. [9] assumed that the electric dipole moment (EDM) of the τ was absent, while Ref. [7], when obtaining bounds for a_τ , assumed that EDM was equal to its SM value, which is negligibly small.

In general, the EDM of the τ lepton, d_τ , can take nonzero values if both the parity P and time reversal T symmetries are violated [10]. In contrast to the interaction of MDM with the magnetic field $\vec{\mathcal{B}}$

$$H_M = -\vec{\mu}_\tau \vec{\mathcal{B}} = -\frac{g_\tau}{2} \mu_B \vec{\sigma} \vec{\mathcal{B}}, \quad (5)$$

where $\mu_B = \frac{e\hbar}{2m_\tau c}$ is the Bohr magneton, the interaction of EDM with the electric field $\vec{\mathcal{E}}$

$$H_E = -\vec{d}_\tau \vec{\mathcal{E}} = -\frac{f_\tau}{2} \mu_B \vec{\sigma} \vec{\mathcal{E}}, \quad (6)$$

is P , T and also CP violating. This causes the interest to the EDM of leptons. In framework of the SM the lepton EDM are extremely small as being originated from the 4-loop diagrams and additionally because of the smallness of CP violation via the CKM matrix [11, 12]. For example, the SM estimation for electron is $d_e \lesssim 10^{-38}$ e·cm, while the τ -lepton EDM can be larger by a factor $\frac{m_\tau}{m_e}$, so that $d_\tau \lesssim 3.5 \cdot 10^{-35}$ e·cm, or $f_\tau \lesssim 1.2 \cdot 10^{-20}$. The currently achieved experimental accuracy [13] cited by PDG [1],

$$-0.22 < \text{Re } d_\tau < 0.45 \quad (10^{-16} \text{ e} \cdot \text{cm}), \quad \text{or} \quad -0.008 < \text{Re } f_\tau < 0.0162, \quad (7)$$

$$-0.25 < \text{Im } d_\tau < 0.008 \quad (10^{-16} \text{ e} \cdot \text{cm}), \quad \text{or} \quad -0.009 < \text{Im } f_\tau < 0.00029, \quad (8)$$

is 18 orders of magnitude worse than the SM prediction. Clearly the SM value is hardly reachable in experiments and therefore any observation of the τ EDM will be indication of additional sources of CP violation beyond the SM.

There have been various proposals to measure the MDM and EDM of the τ lepton. At the LHC, it was suggested in Refs. [14, 15] to obtain constraints on the τ MDM in measurements of the Drell-Yan process. The authors of Ref. [16] discussed the possibility to set the limits on the τ MDM by studying the two-photon production of τ leptons, $\gamma\gamma \rightarrow \tau^+\tau^-$. The process $pp \rightarrow p\gamma^*p \rightarrow p\tau^-\bar{\nu}_\tau q'X$ with almost real photon γ^* is examined in Ref. [17].

In Refs. [18, 19] the potential of future colliders for improvement of the current experimental bounds is investigated. In particular, at the electron-positron linear collider CLIC in the processes $\gamma\gamma \rightarrow \tau^+\tau^-$, $\gamma\gamma \rightarrow \tau^+\tau^-\gamma$, and in the reactions $e^-e^+ \rightarrow e^-\gamma^*e^+ \rightarrow \nu_e\tau^-\bar{\nu}_\tau e^+$ with quasi-real photon and $e^-\gamma \rightarrow \nu_e\tau^-\bar{\nu}_\tau$ with Compton back-scattering photon. The reaction $e^-p \rightarrow e^-\gamma^*\gamma^*p \rightarrow e^-\tau^-\tau^+p$ on the future electron-proton colliders LHeC and FCC-he with high center-of-mass energies and high luminosities is considered in [20].

The authors of Refs. [21, 22] proposed to determine the τ Pauli form factor $F_2(s)$ from the electron-positron annihilation to a pair of tau leptons at the high-luminosity B factory Super-KEKB. The process $e^+e^- \rightarrow \tau^+\tau^-$ is planned to be studied at the Υ resonances $\Upsilon(1S)$, $\Upsilon(2S)$, $\Upsilon(3S)$. This idea was further reconsidered and refined in Ref. [23].

A new method was proposed in Refs. [23, 24] to probe the τ dipole moments from radiative leptonic τ decays $\tau^- \rightarrow \ell^- \nu_\tau \bar{\nu}_\ell \gamma$ ($\ell = e, \mu$) at the KEKB and Super-KEKB colliders. The

feasibility studies [23] show that such a measurement at Belle II will be competitive with the current limits for MDM given in Eq. (3).

Another method to determine the MDM of the τ lepton was discussed in Ref. [25]. It is based on the phenomenon of the particle spin precession in a bent crystal. This method has been successfully used by the E761 collaboration at Fermilab [26] to measure the MDM of the Σ^+ hyperon. The authors of [25] discussed the decay $B^+ \rightarrow \tau^+ \nu_\tau$ as a source of polarised τ leptons. However, the branching fraction of this decay is only about 10^{-4} which can make realization of this idea practically difficult.

Nevertheless, the method which uses channeling of short-lived baryons in bent crystals has recently attracted considerable attention [27–31]. In particular, in Ref. [28] the feasibility of measuring the MDM of the charm baryons Λ_c^+ and Ξ_c^+ at the LHC was addressed (see also details in Ref. [32]). The authors of [29, 30] studied the application of this method for future measurements of EDM and MDM of the strange, charm and beauty baryons.

In the present paper we would like to propose the idea of measuring the MDM and possibly EDM of the τ lepton through its spin precession in a bent crystal. We suggest to use polarised τ leptons which come from the decay of the D_s mesons produced at the LHC. Because of the quark structure of D_s meson ($D_s^+ = c\bar{s}$), the branching fraction of interest is quite sizeable, $\mathcal{B}(D_s^+ \rightarrow \tau^+ \nu_\tau) = 0.0548(23)$ [1].

The D_s mesons are produced in pp collisions with very high energies, of a few TeV, and subsequently decay to polarised τ leptons. The leptons can be directed into a bent crystal, get in the channeling regime, and the direction of τ polarisation after the precession in the crystal can be determined from the angular analysis of its decay products. Schematically, the whole process is

$$pp \rightarrow D_s^+ X, \quad D_s^+ \rightarrow \tau^+ \nu_\tau, \quad \tau^+ \text{ flight in the crystal}, \quad \tau^+ \rightarrow \pi^+ \pi^+ \pi^- \bar{\nu}_\tau. \quad (9)$$

For the present study we consider the τ decay into three charged pions, which allows to identify the τ lepton through the reconstruction of a secondary vertex. The various aspects of this measurement are studied in the present paper.

II. PRINCIPLE OF THE MEASUREMENT

A. Initial polarisation of τ leptons from D_s decays

In pp collisions the τ leptons are mainly produced in the decay $D_s^+ \rightarrow \tau^+ \nu_\tau$, with a polarisation vector (see details in Appendix A)

$$\vec{\mathbb{P}} = \frac{1}{M_D k_\tau^*} \left[m_\tau \vec{p}_D - E_D \vec{k}_\tau + \frac{\vec{k}_\tau (\vec{k}_\tau \cdot \vec{p}_D)}{m_\tau + \varepsilon_\tau} \right]. \quad (10)$$

Here (E_D, \vec{p}_D) is the four-momentum of D_s meson, $(\varepsilon_\tau, \vec{k}_\tau)$ is the four-momentum of τ lepton in the lab frame, and $k_\tau^* = (M_D^2 - m_\tau^2)/(2M_D)$ is the momentum of τ lepton in the rest frame of the D_s meson.

It is convenient to separate the longitudinal and transverse components of the polarisation vector with respect to the direction of motion of the τ lepton,

$$\begin{aligned} \vec{\mathbb{P}}_{\parallel} &= \frac{1}{M_D k_\tau^*} (\varepsilon_\tau p_D \cos \theta - E_D k_\tau) \vec{n}_k, \\ \vec{\mathbb{P}}_{\perp} &= \frac{m_\tau p_D}{M_D k_\tau^*} (\vec{n}_p - \vec{n}_k \cos \theta), \end{aligned} \quad (11)$$

where we defined unit vectors $\vec{n}_k \equiv \vec{k}_\tau/k_\tau$ and $\vec{n}_p \equiv \vec{p}_D/p_D$, and $\cos \theta = \vec{n}_k \vec{n}_p$. These components are not independent and satisfy

$$\vec{\mathbb{P}}_{\parallel}^2 + \vec{\mathbb{P}}_{\perp}^2 = 1, \quad (12)$$

$$|\vec{\mathbb{P}}_{\perp}| = \frac{m_\tau p_D}{M_D k_\tau^*} \sin \theta. \quad (13)$$

It is seen from Eqs. (12) and (13) that if the τ lepton moves in the direction of the D_s meson, i.e. $\theta = 0$, then the polarisation is purely longitudinal and $|\vec{\mathbb{P}}_{\parallel}| = 1$. The transverse polarisation increases with increasing θ and takes its maximal value $|\vec{\mathbb{P}}_{\perp}| = 1$ at the maximal allowed angle determined from

$$\sin \theta_{max} = \frac{M_D k_\tau^*}{m_\tau p_D} = \frac{\gamma_\tau^* v_\tau^*}{\gamma_D v_D}, \quad (14)$$

where $\vec{v}_D = \vec{p}_D/E_D$ is velocity of the D_s meson in the lab frame, $\vec{v}_\tau^* = \vec{k}_\tau^*/\varepsilon_\tau^*$ is velocity of the τ lepton in the rest frame of the D_s meson, and the corresponding Lorentz factors are $\gamma_D = E_D/M_D$ and $\gamma_\tau^* = \varepsilon_\tau^*/m_\tau$. Figure 1 shows schematically the ellipsoid of the τ momenta and the behavior of the τ polarisation.

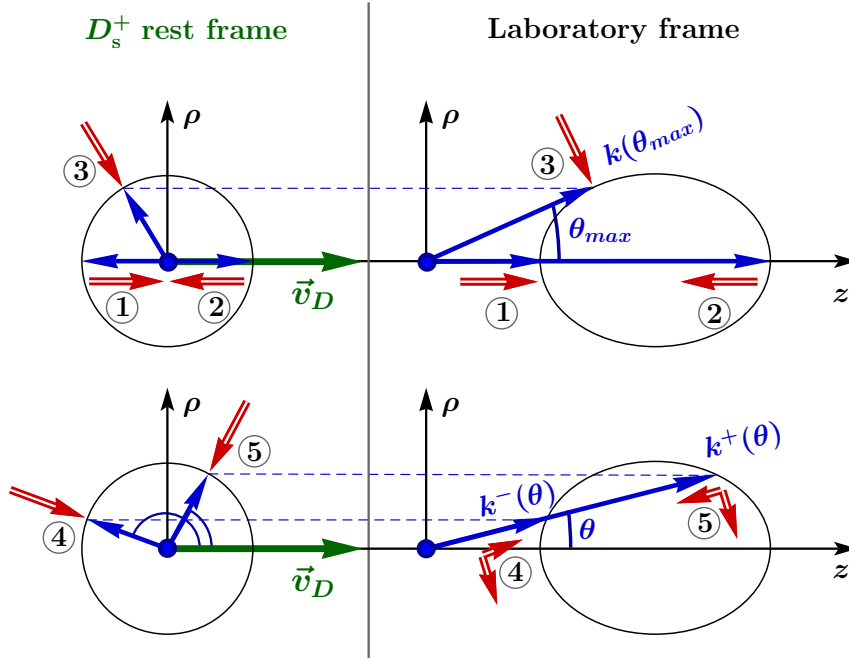


FIG. 1. The decay $D_s^+ \rightarrow \tau^+ \nu_\tau$ in the (left) D_s rest frame and (right) Lab frame. The axis Oz is chosen along the direction of D_s momentum. Rotational symmetry around the Oz axis is implied. The ellipsoid is actually very elongated along the axis Oz because $\gamma_D \gg 1$. The blue arrows show the τ momentum \vec{k}_τ , and the thick red arrows the τ polarisation vector, $\vec{\mathbb{P}}$. Several cases of τ polarisation in the Lab frame are shown: (1,2) $\theta = 0$, (3) $\theta = \theta_{max}$ and (4,5) an arbitrary θ .

At the minimal τ energy,

$$\varepsilon_\tau^-(\theta = 0) = \frac{1}{M_D} (E_D \varepsilon_\tau^* - p_D k_\tau^*) \approx \frac{m_\tau^2}{M_D^2} E_D, \quad (15)$$

the polarisation is longitudinal and $\vec{\mathbb{P}}_\parallel = +\vec{n}_z$, while at the maximal τ energy,

$$\varepsilon_\tau^+(\theta = 0) = \frac{1}{M_D} (E_D \varepsilon_\tau^* + p_D k_\tau^*) \approx E_D, \quad (16)$$

the polarisation is longitudinal and $\vec{\mathbb{P}}_\parallel = -\vec{n}_z$. At the τ energy corresponding to the maximal angle θ_{max} ,

$$\varepsilon_\tau^+(\theta_{max}) = \varepsilon_\tau^-(\theta_{max}) = \frac{2m_\tau^2}{M_D^2 + m_\tau^2} E_D, \quad (17)$$

the polarisation is purely transverse and $|\vec{\mathbb{P}}_\perp(\theta_{max})| = 1$.

We can rewrite the expressions for the longitudinal and transverse τ polarisations, Eq. (11), as functions of the τ and D_s energies, assuming $\varepsilon_\tau = k_\tau$, as we consider only energetic τ leptons,

$$\vec{P}_{\parallel}(E_D, \varepsilon_{\tau}) \approx - \frac{\frac{M_D^2 + m_{\tau}^2}{2m_{\tau}^2} - \frac{E_D}{\varepsilon_{\tau}}}{\frac{M_D^2 + m_{\tau}^2}{2m_{\tau}^2} - 1} \vec{n}_k,$$

$$|\vec{P}_{\perp}(E_D, \varepsilon_{\tau})| \approx \frac{2m_{\tau}^2}{M_D^2 - m_{\tau}^2} \sqrt{\left(\frac{M_D^2}{m_{\tau}^2} - \frac{E_D}{\varepsilon_{\tau}}\right) \left(\frac{E_D}{\varepsilon_{\tau}} - 1\right)}. \quad (18)$$

Figure 2 presents the transverse and longitudinal polarisations of Eq. (18) of τ leptons produced by D_s mesons of energy $E_D = 2$ TeV, as a function of the τ energy.

The blue dashed line shows the τ spectra, which in the relativistic case is a step function. Due to a small asymmetry (see Fig. 2, left) there is a small average longitudinal polarisation of the order of 10% in the direction $-\vec{n}_z$.

Note, that due to a cylindrical symmetry, τ leptons produced from D_s decays of the same energy at the same polar angle θ but with opposite azimuthal angles, ϕ and $\phi + \pi$, would have an almost opposite transverse polarisation,

$$\vec{P}_{\perp}(\theta, \phi) \approx -\vec{P}_{\perp}(\theta, \phi + \pi). \quad (19)$$

Thus, for the sufficient precision at the τ polarisation analysis, the directions of the D_s and τ momenta should be known with a precision better than θ_{max} .

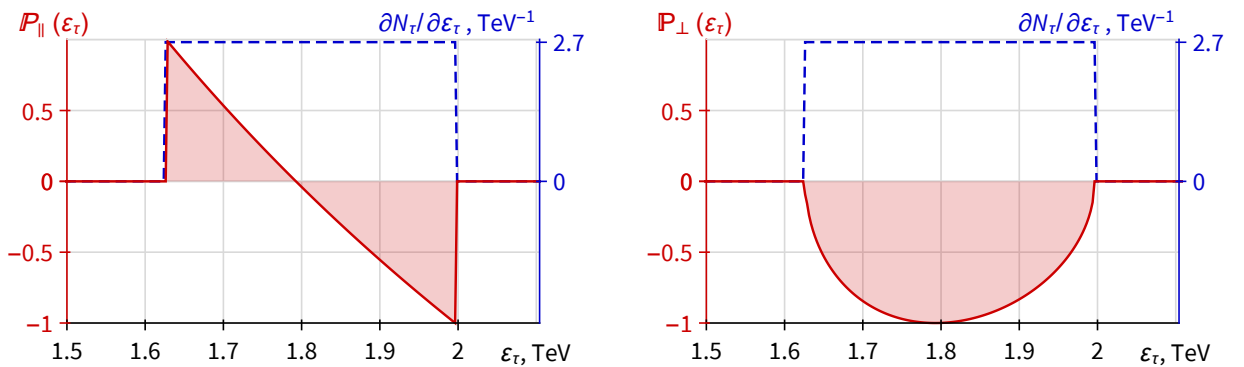


FIG. 2. (Left) Longitudinal and (right) transverse polarisations as a function of the energy of τ leptons produced by 2 TeV D_s mesons. The red solid line is the polarisation and the blue dashed line is the τ spectrum.

TABLE I. Several τ hadronic decay channels with asymmetry parameter, α , and sensitivities. Sensitivities, S , are shown for the measurements made with different number of observables, \vec{n}_k is the direction of τ momentum. Columns 2,3 and 4 are our calculations and columns 5, 6, 7 and 8 are from the analysis of Ref. [33].

| τ decay | α | α_{eff} | $S(1)_{\text{eff}}$ | S(1) | $S(2)$ | S(all but \vec{n}_k) | S(with \vec{n}_k) |
|---|----------|-----------------------|---------------------|------|--------|-------------------------|----------------------|
| $\tau^+ \rightarrow \pi^+ \bar{\nu}_\tau$ | 1 | 1 | 0.58 | 0.58 | – | 0.58 | 0.58 |
| $\tau^+ \rightarrow \rho^+ (2\pi) \bar{\nu}_\tau$ | 0.45 | 0.49 | 0.28 | 0.26 | 0.49 | 0.49 | 0.58 |
| $\tau^+ \rightarrow a_1^+ (3\pi) \bar{\nu}_\tau$ | 0.021 | 0.12–0.21 | 0.069–0.12 | 0.10 | 0.23 | 0.45 | 0.58 |

B. Final polarisation and energy of reconstructed τ leptons

Let us discuss possibilities to measure the τ polarisation. In general, it can be obtained from the angular distribution of the final particles in the τ decays. In a two-body decay, this distribution has the form

$$\frac{1}{N} \frac{dN}{d\Omega} = \frac{1}{4\pi} \left(1 + \alpha \vec{\mathbb{P}} \cdot \vec{n} \right), \quad (20)$$

where $\vec{n} \equiv \vec{p}/p$ is the unit vector in the direction of movement of the final particle-analyzer and α is the asymmetry parameter. Several hadronic decay channels can be considered. They are listed in Table I.

In the second column, the parameter α for the two-body decay is given. Other columns contain information on the sensitivity $S = 1/(\sigma\sqrt{N})$ to the polarisation, where N is the number of events, σ is the error on polarization measurement at $\vec{\mathbb{P}} = 0$. According to Ref. [33] if the full kinematics of the decay is reconstructed then the maximum possible sensitivity $S = 1/\sqrt{3} \approx 0.58$ is reached.

For the single-pion channel, the maximum sensitivity is achieved, even though this channel suffers from large background. For the vector-meson channels, the sensitivity is suppressed because of the smaller asymmetry parameter $\alpha = (m_\tau^2 - 2m_v^2)/(m_\tau^2 + 2m_v^2)$ ($m_v = m_\rho, m_{a_1}$). The parameter α for the $a_1(1260)$ meson turns out to be 0.021 which leads to the low sensitivity about 0.01. However we can estimate the influence of the large decay width of this resonance. For this, we integrate α as a function of the invariant mass W of a resonance, weighted with a normalised Breit-Wigner distribution,

$$\alpha_{\text{eff}} = \int_0^{m_\tau} \left(\frac{m_\tau^2 - 2W^2}{m_\tau^2 + 2W^2} \right) \frac{dW}{(W^2 - m_v^2)^2 + m_v^2 \Gamma_v^2} \left(\int_0^{m_\tau} \frac{dW}{(W^2 - m_v^2)^2 + m_v^2 \Gamma_v^2} \right)^{-1}. \quad (21)$$

Choosing $m_{a_1} = 1230$ MeV and the decay width $\Gamma_{a_1} = 250 - 600$ MeV [1], we obtain an interval for the effective parameter for the $a_1(1260)\nu_\tau$ mode in the third column of Table I. The corresponding sensitivity is given in the fourth column. It is seen that accounting for the large decay width of $a_1(1260)$ enhances the sensitivity considerably. For the $\rho\nu_\tau$ mode, the effect of the width is much less important as seen also in Table I.

The analysis of Ref. [33] shows that the sensitivity of the polarisation measurement increases with increasing the number of observables, and reaches the maximal value of 0.58 if, in addition, the direction of the τ momentum is determined. Thus one can opt for the 3-prong decay $\tau^+ \rightarrow a_1^+ \bar{\nu}_\tau \rightarrow \pi^+\pi^+\pi^-\bar{\nu}_\tau$ as it can be separated from background processes and allows us to reconstruct the position of the vertex. Note that various aspects of the $\tau \rightarrow 3\pi\nu_\tau$ decay mode are studied in Refs. [34–36].

In this paper we do not address the reconstruction of τ polarisation, but an estimation on sensitivity. The sensitivity on polarisation in $\tau^+ \rightarrow a_1^+ \bar{\nu}_\tau$ decay is very small $S \sim 0.1$. On the other hand, if we also analyse the consequent decay $a_1^+ \rightarrow \pi^+\pi^+\pi^-$ the sensitivity reaches its maximal possible value $S \sim 0.58$. Thus, a big part of sensitivity comes from a_1 , which can be fully reconstructed, so we can safely estimate that $S > 0.2$.

For this reason in the sensitivity studies (in Sec. III) we chose to use the range for sensitivity on polarisation ($0.2 < S < 0.58$).

The energy of τ can be partially reconstructed. Assuming that we fully reconstruct a_1 from $a_1^+ \rightarrow \pi^+\pi^+\pi^-$ decay, using the relation between energies of a_1 and τ , that is analogous to the ones shown in Eq. (15) and (16), we obtain the relative error on τ energy

$$\frac{\Delta\varepsilon_\tau}{\varepsilon_\tau} = \frac{1}{\sqrt{3}} \frac{m_\tau^2/m_{a_1}^2 - 1}{m_\tau^2/m_{a_1}^2 + 1} \approx 0.21. \quad (22)$$

Of course, putting the additional silicon telescope detector in front of the crystal could allow to fully reconstruct the decay kinematics, but this setup would require a detailed study of the background in the environment where the experiment will be located.

C. Experimental setup

When a relativistic τ lepton is deflected by a bent crystal, its polarisation vector rotates by an angle which is proportional to the anomalous MDM [28, 37–39],

$$\angle(\vec{\mathbb{P}}_i, \vec{\mathbb{P}}_f) = (1 + \gamma_\tau a_\tau) \Theta, \quad (23)$$

where $\vec{\mathbb{P}}_i$ and $\vec{\mathbb{P}}_f$ are the vectors of the initial and final polarisations of τ lepton (before and after the crystal), γ_τ is the Lorentz factor of τ lepton ($\gamma_\tau \gg 1$), and $\Theta = L/R$ is the deflecting angle of the bent crystal, L and R being the length and bending radius of the crystal.

Thus, to measure the anomalous MDM of τ we need to have a beam of polarised τ leptons directed at the crystal, and to know the τ initial and final polarisations and energy. As the polarised τ leptons are produced from the decay of D_s mesons, the crystal should be placed at a certain distance L_V from the target to maximise the probability of τ production (see Appendix B).

To reconstruct the direction of initial polarisation of Eq. (11), we need to select τ leptons coming from D_s decays and also to know the direction of the D_s and τ momenta and the energy of either D_s or τ particles. For the present study we consider the τ decay into three charged pions, so we need a suitable setup in order to get rid of the background processes leading to the same final state (see Sec. III C). A solution could be to put a silicon telescope detector between the target and the crystal (see Fig. 3). Further optimisation of the telescope design can be performed, however, the outlined structure is sufficient for a demonstration of the measurement principle, which is a purpose of the present article.

The first problem of this setup is that the telescope detector should have a very high angular

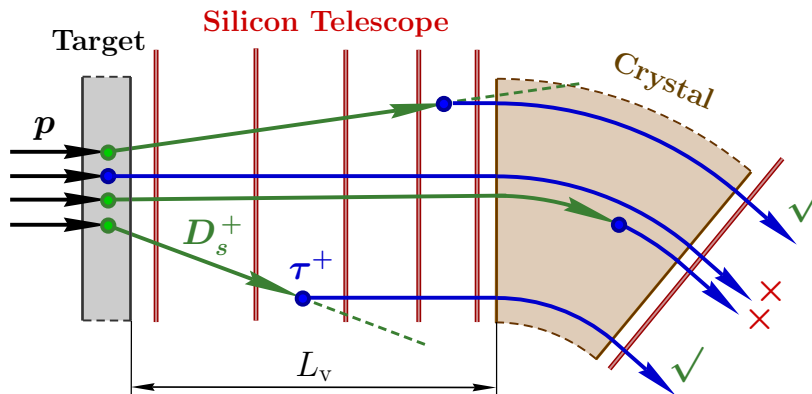


FIG. 3. Schematics of the setup with a silicon telescope detector.

resolution on a rather short base: the distance between the target and the crystal should be $\sim 10 - 40$ cm (see Appendix B), and the angular resolution should be better than $\theta_{max}(E_D = 2 \text{ TeV}) \approx 100 \mu\text{rad}$. The second problem is that the telescope detector in this case is very close to the target and could suffer from the background overload.

In this concern, we propose a two crystal setup as shown in Fig. 4. The purpose of the first crystal is to channel D_s mesons and so to constrain their momentum direction. Misaligning the first crystal from the direction of the proton beam by a small angle θ_p is to restrict the channeling of the initial protons. As a result we would have a collimated beam of D_s^+ mesons satisfying the condition $|\theta_x| < \theta_{acc} \sim 5 \mu\text{rad}$, where $\theta_x = \arcsin(p_x/p)$ and θ_{acc} is the angle of acceptance to the planar channeling regime [28, 32].

The second crystal is for channeling the τ lepton from the D_s decay. Misaligning the second crystal from the direction of the D_s beam by an angle θ_v would select (by channeling) only τ leptons produced between the two crystals and would not permit the collimated D_s beam to be channeled in the second crystal (see Fig. 4). The initial direction of the τ polarisation is reconstructed from the D_s and τ momenta, which are selected by channeling in the first and the second crystal, respectively.

In the following, we will determine the optimal parameters of this setup: lengths and bending radii of two crystals, distance between crystals and orientation of the second crystal. The direction of the final polarisation can be reconstructed by analysing the angular distribution of the τ decay products, as we discussed in Sec. II B. Finally, we obtain from (23) the value of the anomalous MDM a_τ .

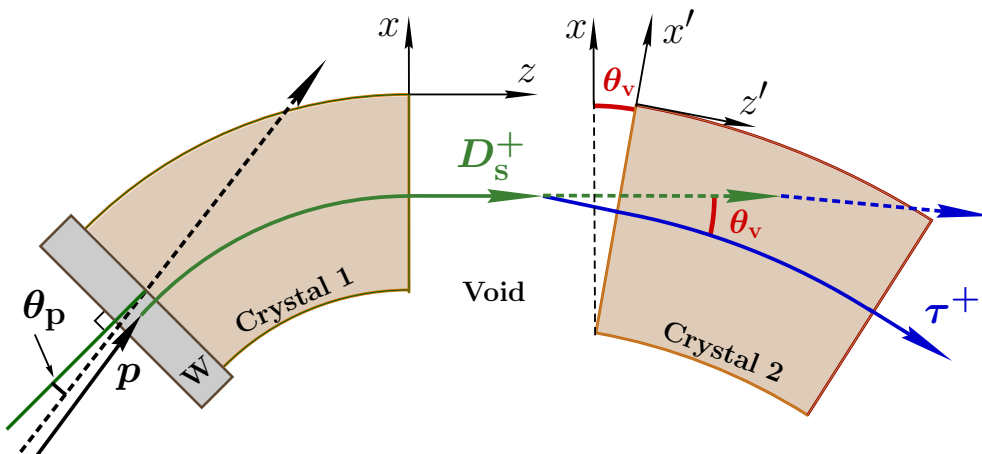


FIG. 4. Double crystal scheme.

III. SENSITIVITY STUDIES

In this section we present a sensitivity study for measuring the MDM and EDM of the τ lepton using the setup described in the previous section. The absolute statistical error of the measurement of the anomalous magnetic moment can be written in the following way,

$$\Delta a_\tau = \sqrt{\frac{1}{N_{\text{POT}} \eta_{\text{det}} Br S^2 \eta_{\text{setup}}}}, \quad \eta_{\text{setup}} = \Theta^2 \int d\varepsilon \frac{\partial N_\tau^{\text{def}}}{\partial \varepsilon} \gamma_\tau^2 \mathbb{P}^2, \quad (24)$$

where N_{POT} is the total number of protons on target, η_{det} is the detector efficiency, Br is the branching fraction of the selected τ decay, S is the sensitivity of polarisation reconstruction by the analysis of the τ decay, η_{setup} is the setup efficiency (target plus two crystals), $\partial N_\tau^{\text{def}}/d\varepsilon$ is the spectrum of deflected τ leptons normalised to one initial proton, γ_τ and $\mathbb{P}^2 = \mathbb{P}_x^2 + \mathbb{P}_z^2$ are the Lorentz factor and the square of averaged polarisation (in xz plane) of the deflected τ lepton as a function of its energy. In the following sections, we discuss these terms and give some estimates on their values.

The error of MDM connected with the precision of τ energy reconstruction (22) can be written in the following way,

$$\Delta a^{(\gamma)} = \frac{\bar{a} + \gamma^{-1}}{1 + \gamma/\Delta\gamma} \approx \frac{\bar{a}_\tau + 0.001}{6}. \quad (25)$$

Considering the expected value of anomalous MDM, $\bar{a}_\tau \sim 0.001$ and Lorentz factor, $\gamma \sim 1000$ this contribution is negligible.

Due to the MDM, the spin precession takes place only in the xz plane. If τ lepton possesses the EDM, the y component of polarisation will also be induced. In the limit $\gamma_\tau \gg 1$, and assuming that EDM effects are small compared to the MDM spin precession, using formulas in [30], the ratio between absolute error on EDM and MDM is

$$\frac{\Delta f_\tau}{\Delta a_\tau} \approx \left| \frac{4\gamma\bar{a}_\tau}{\Theta(1 + \gamma\bar{a}_\tau)^2} \right| \quad (26)$$

Analogous to (24) the absolute statistical error of the measurement of the EDM can be written in the following way,

$$\Delta f_\tau = \sqrt{\frac{1}{N_{\text{POT}} \eta_{\text{det}} Br S^2 \eta_{\text{setup}}^{(f)}}}, \quad \eta_{\text{setup}}^{(f)} = \frac{\Theta^4}{16\bar{a}_\tau^2} \int d\varepsilon \frac{\partial N_\tau^{\text{def}}}{\partial \varepsilon} (1 + \gamma_\tau \bar{a}_\tau)^4 \mathbb{P}^2, \quad (27)$$

A. First crystal: spectrum of deflected D_s mesons

The spectral angular distribution of D_s mesons produced by 7 TeV protons on a fixed target is obtained simulating minimum-bias pp collisions with the Pythia 8.2 generator [40] and shown in Fig. 5. In the current study we choose a tungsten target with depth $L_{\text{tar}} = 1$ cm along the direction of the incident proton beam. As it was shown in Ref. [28], the target depth is limited only by the increasing number of secondary particles produced in deeper targets.

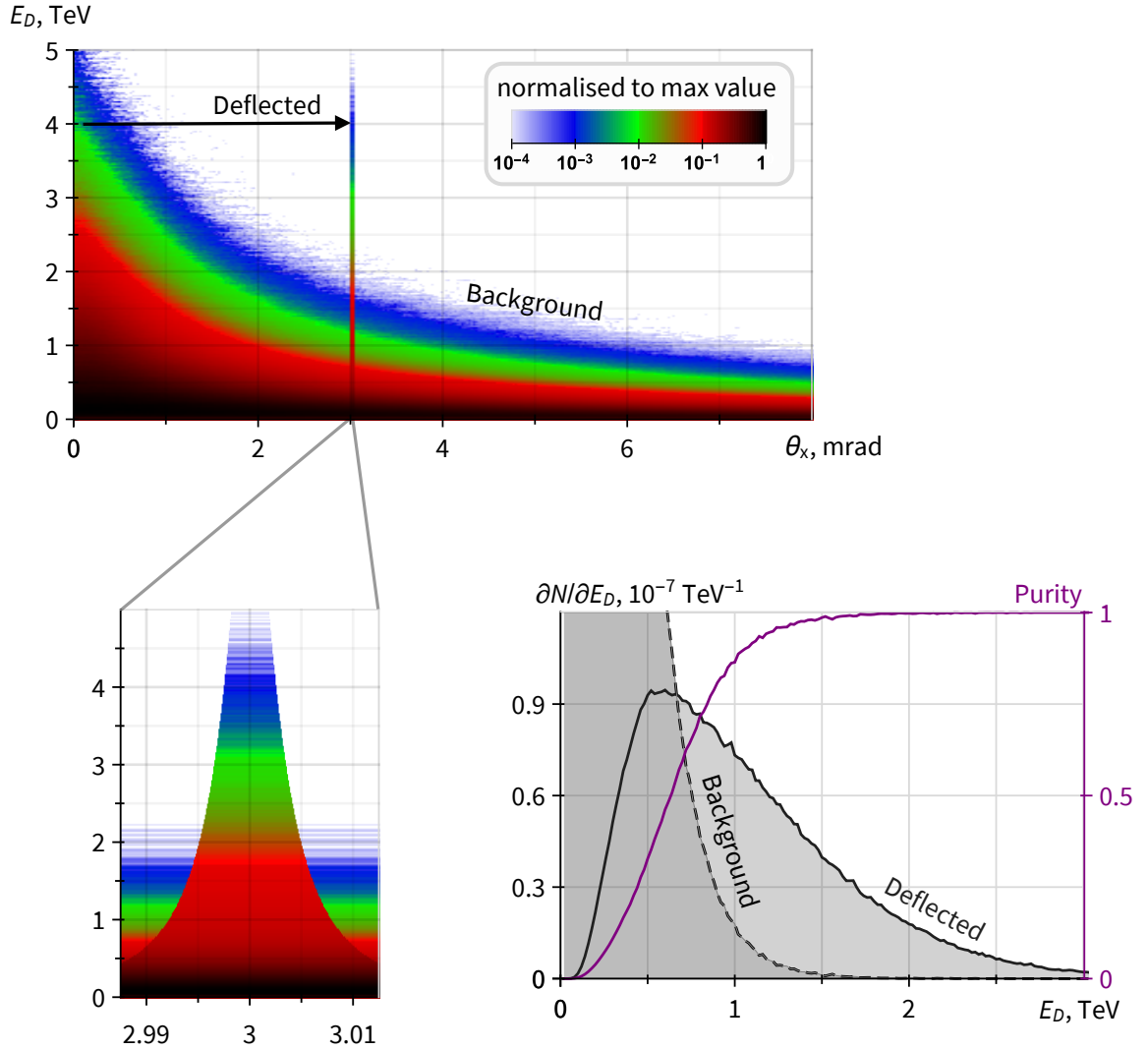


FIG. 5. Spectral angular distribution of D_s mesons after the first crystal. “Deflected” describes a collimated D_s beam deflected by a germanium crystal by $\Theta_D = 3$ mrad; “Background”, D_s^+ produced in the target. Purity is the ratio of deflected D_s^+ to all D_s^+ mesons (initially produced or deflected) at θ_x . $\theta_x = 0$ corresponds to the direction of proton beam.

Assuming no nuclear effects the production rate of D_s^+ mesons per one incident proton is

$$N_D^{\text{tar}} = \rho N_A \sigma_D \frac{A_{\text{tar}}}{M_{\text{tar}}} L_{\text{tar}}, \quad (28)$$

where ρ , A_{tar} and M_{tar} are the density, number of nucleons and molar mass of the target, respectively, N_A is the Avogadro number, and σ_D is the cross section of D_s^+ production in pp collision at center-of-mass energy $\sqrt{s} = 115 \text{ GeV}$ (corresponding to the fixed target experiment at the 7 TeV LHC proton beam). For the chosen target, $N_D^{\text{tar}} \approx 1.4 \times 10^{-4}$.

In the setup shown in Fig. 4, we propose to place a crystal with the purpose of preparing a collimated energetic beam of D_s mesons. The initial direction of the crystallographic plane is chosen as $\theta_p = 100 \mu\text{rad}$. Thus, after the first crystal, we can have two categories of D_s meson beams. The first one, referred from now on as ‘‘Background’’, is composed of D_s^+ mesons which are initially produced at an angle $\theta_x \sim \Theta_D$. In this case, the D_s mesons are poorly collimated, and as a consequence, the average τ polarisation is close to zero. The second category, further referred as ‘‘Deflected’’, is composed of D_s^+ mesons deflected by the crystal by an angle Θ_D . These D_s mesons are collimated and hence can be the source of polarised τ leptons.

The purity, which is defined as the ratio between the number of deflected D_s mesons and the total (‘‘Background’’+‘‘Deflected’’) number of D_s mesons, is increasing as a function of energy as can be seen on Fig. 5. For the sensitivity analysis, we take into account this effect by introducing an effective spectra, which is obtained by convolution of the spectra with the purity. The background from the D_s produced at Θ_D is specifically considered, while a preliminary consideration of other sources is addressed in section III C.

The spectral angular distribution of D_s mesons deflected by a bent crystal (Fig. 5, Deflected) is obtained using a parameterisation based on the Monte Carlo simulation of particle propagation through the crystal [32], accounting the incoherent scattering on the electron subsystem of a crystal and on thermal vibrations of the atoms at lattice nodes, that leads to dechanneling effect. The optimal bending radii and lengths were found for a silicon crystal to be $R_D = 15 \text{ m}$ and $L_D = 4.5 \text{ cm}$, and for a germanium crystal, $R_D = 10 \text{ m}$ and $L_D = 3 \text{ cm}$. Thus, the optimal deflection angle is $\Theta_D \sim 3 \text{ mrad}$. From our simulation, we determined that the D_s deflection rate per one incident proton on target by a germanium crystal is about 1.1×10^{-7} and about 0.6×10^{-7} with a silicon crystal.

B. Second crystal: spectrum and polarisation of deflected τ leptons

For an optimal rate of τ leptons from D_s decays, the second crystal should be placed at a distance $L_v \sim 10$ cm from the first one (see Appendix B). This way, about 1.3 % of D_s mesons will decay into τ leptons before the entrance of the second crystal.

The momentum distribution of the τ leptons produced in the two-body decay is defined by the momentum of the D_s mesons. In the laboratory frame, the τ momenta form an ellipsoid of rotation. Figure 6 represents the τ momentum distribution in the $p_x p_z$ and $p_y p_z$ phase spaces in the laboratory frame. The two red lines at the angles $\theta_v \pm \theta_{acc}$ from the p_z -axis highlight the area of phase space of τ momentum that can be deflected by the second crystal. In $p_y p_z$ phase space the deflected area has an elliptical shape which results from intersection of the second crystal plane with the ellipsoid of the τ momenta.

As can be seen from the figure, the misalignment of the two crystals leads to a large suppression of the spectra of deflected τ leptons. For instance, the angle between the crystals $\theta_v = 100 \mu\text{rad}$ (see Fig. 4) matches the maximal allowed angle between the τ and D_s momenta given in Eq. (14) for a D_s energy of $E_D = 2$ TeV, thus, τ leptons produced by more energetic D_s mesons would not be deflected. Nevertheless, the deflected τ leptons produced by 2 TeV D_s mesons would be almost

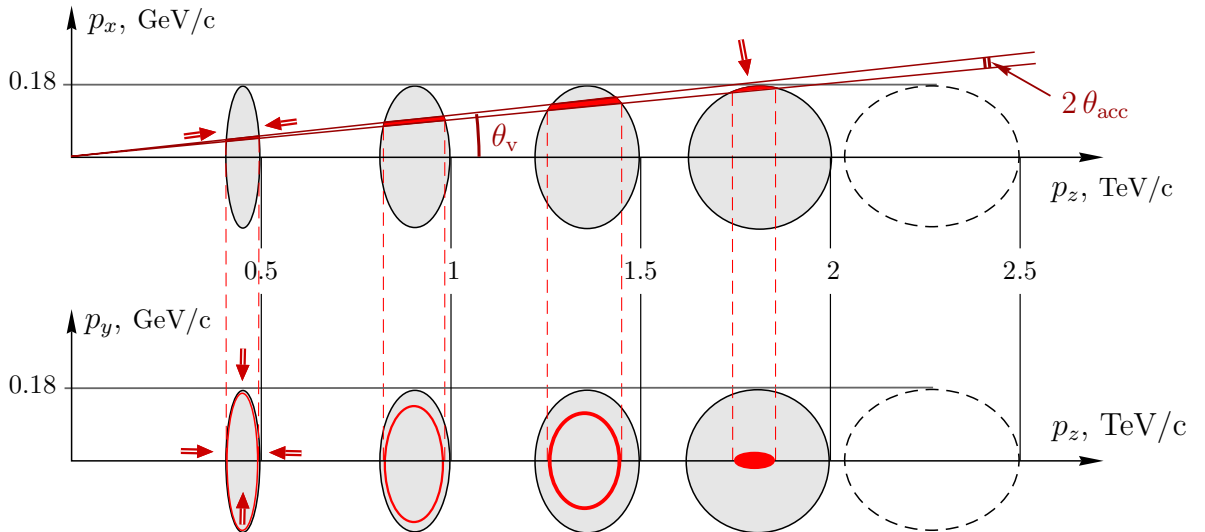


FIG. 6. Collimation of τ momenta by the second crystal. p_z is chosen in the direction of the D_s momentum. Each ellipsoid represents the phase space of τ leptons produced by D_s mesons of specific energy. The red area shows the phase space of τ leptons collimated by the second crystal. Arrows show the polarisation of τ . Scale on p_x is $\sim 10^4$ times smaller than on p_z because $\gamma_D \gg 1$.

100% polarised in the x direction, unlike those produced by less energetic D_s mesons as can be seen in Fig. 6.

The spectra of deflected τ leptons can be described by the following expression

$$\frac{\partial N_\tau^{\text{def}}}{\partial \varepsilon_\tau} = \int_0^{\varepsilon_{\text{max}}} dE_D \frac{\partial N_D}{\partial E_D} \eta(L_v, E_D) \frac{\partial N_\tau}{\partial \varepsilon_\tau}(E_D) \eta_{\text{coll}}(E_D, \varepsilon_\tau) \eta_{\text{chan}}(\varepsilon_\tau), \quad (29)$$

where $\partial N_D/\partial E_D$ is the effective spectra of deflected D_s mesons (accounting for the purity), $\eta(L_v, E_D)$ is the conversion efficiency of D_s^+ into τ^+ given in Eq. (B3), $\partial N_\tau/\partial \varepsilon_\tau(E_D)$ is the spectra of τ leptons produced by D_s decays as a function of the D_s energy, $\eta_{\text{chan}}(\varepsilon_\tau)$ is the channeling efficiency [32] taking into account the τ decay, $\eta_{\text{coll}}(E_D, \varepsilon_\tau) = (\phi_{\text{max}} - \phi_{\text{min}})/\pi$ is the fraction of τ leptons collimated when entering the crystal, with

$$\sin \phi = \frac{\theta_x}{\theta(E_D, \varepsilon_\tau)}, \quad \sin \phi_{\text{max}} = \frac{\theta_v + \theta_{\text{acc}}(\varepsilon_\tau)}{\theta(E_D, \varepsilon_\tau)}, \quad \sin \phi_{\text{min}} = \frac{\theta_v - \theta_{\text{acc}}(\varepsilon_\tau)}{\theta(E_D, \varepsilon_\tau)}. \quad (30)$$

The expressions for the projections of polarisation on the x and z axes in the relativistic case are

$$\mathbb{P}_x(E_D, \varepsilon_\tau, \phi) = \mathbb{P}_\perp(E_D, \varepsilon_\tau) \sin \phi, \quad \mathbb{P}_z(E_D, \varepsilon_\tau) \approx \mathbb{P}_\parallel(E_D, \varepsilon_\tau). \quad (31)$$

By averaging over the D_s spectra and taking into account the collimation due to channeling, we get the expression of the x and z components of polarisation of deflected τ leptons as a function of energy,

$$\mathbb{P}_z(\varepsilon_\tau) = \frac{1}{\partial N_\tau^{\text{def}}/\partial \varepsilon_\tau} \int dE_D \frac{\partial N_D}{\partial E_D} \frac{\partial N_\tau^{\text{def}}}{\partial \varepsilon_\tau}(E_D) \mathbb{P}_z(E_D, \varepsilon_\tau), \quad (32)$$

$$\mathbb{P}_x(\varepsilon_\tau) = \frac{1}{\partial N_\tau^{\text{def}}/\partial \varepsilon_\tau} \int dE_D \frac{\partial N_D}{\partial E_D} \frac{\partial N_\tau}{\partial \varepsilon_\tau}(E_D) \mathbb{P}_\perp(E_D, \varepsilon_\tau) \frac{1}{\pi} \int_{\phi_{\text{min}}(\varepsilon_\tau)}^{\phi_{\text{max}}(\varepsilon_\tau)} \sin \phi \, d\phi. \quad (33)$$

The integration over ϕ in Eq. (33) means averaging over the direction of particles in crystal plane and over acceptance angle in the direction perpendicular to this plane. In Eq. (32) this integration is trivial, and is simply the term η_{coll} from Eq. (29). Due to the symmetry of the setup the average of y -component of the initial polarisation is zero.

In Fig. 7 we present the spectra given in Eq. (29) and the polarisation as a function of energy given in Eqs. (32) and (33) of deflected by 12 cm germanium crystal τ leptons for two orientations of the second crystal, (left) $\theta_v = 40 \mu\text{rad}$, $R = 9 \text{ m}$, and (right) $\theta_v = 80 \mu\text{rad}$, $R = 7 \text{ m}$.

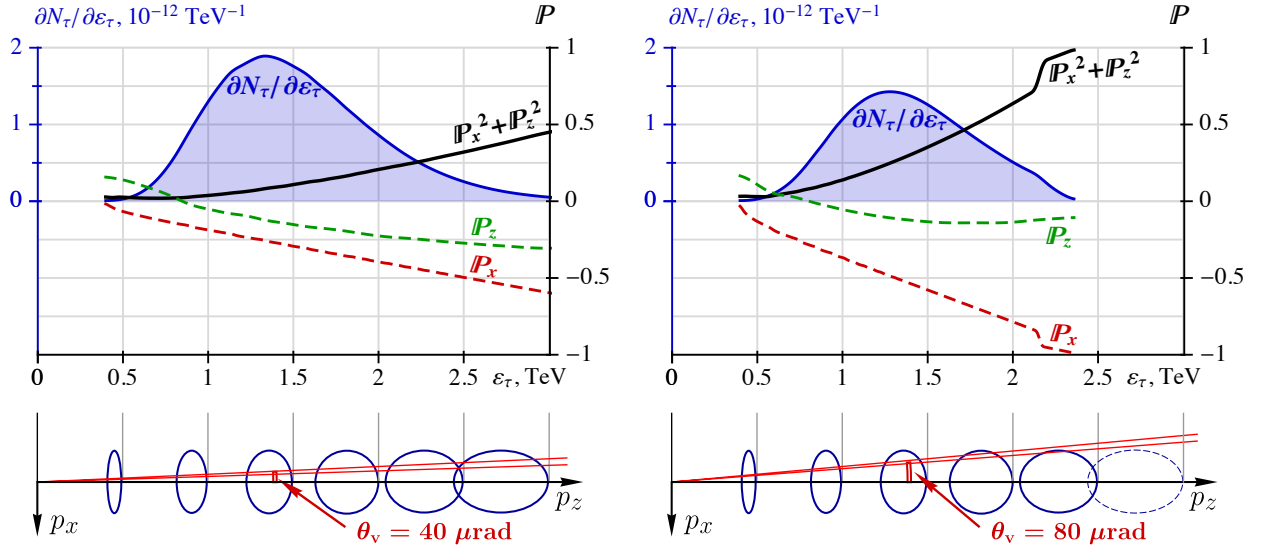


FIG. 7. Polarisation and spectra of deflected τ leptons for (left) $\theta_v = 40 \mu\text{rad}$ and (right) $\theta_v = 80 \mu\text{rad}$. The spectra are normalised to one initial proton. The red and green dashed lines represents the x and z components of the averaged τ polarisation.

In the second case, the number of deflected τ leptons is smaller and the spectra is softer, but the degree of polarisation is significantly greater.

By varying the orientation and dimensions of the second crystal, we find the maximal setup efficiency for MDM measurement, $\eta_{\text{setup}} \sim 1.1 \times 10^{-10}$ per incident proton (see Fig. 8, left). For this case, the second crystal parameters are the following: material — germanium, orientation angle $\theta_v = 80 \mu\text{rad}$, length $L = 10 \text{ cm}$ and bending radius $R = 7 \text{ m}$ and deflection angle $\Theta \approx 14 \text{ mrad}$. If

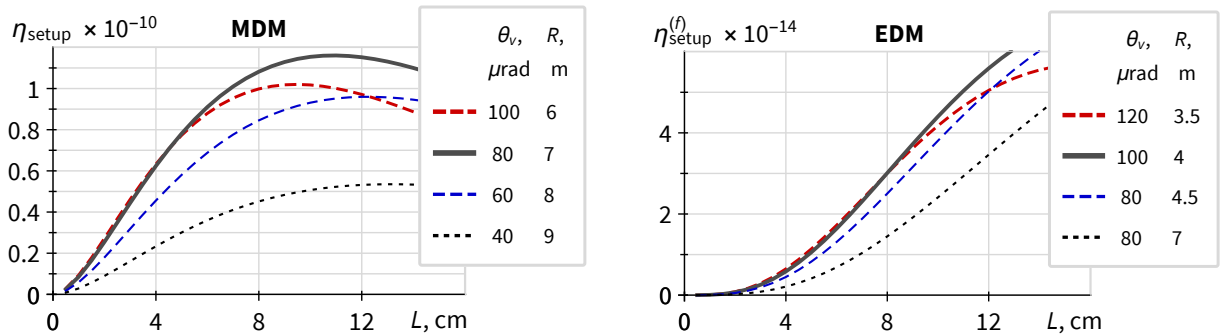


FIG. 8. Setup efficiencies (left) for MDM measurement η_{setup} and (right) for EDM measurement $\eta_{\text{setup}}^{(f)}$ as a function of the second crystal length, L , for various values of the angle θ_v and optimal radii of curvature R (listed on the right).

the crystal length is limited to 6 cm, it is better to increase the orientation angle to $\theta_v = 100 \mu\text{rad}$, so that the optimal bending radius will decrease to $R = 6 \text{ m}$, and hence the deflection angle would be $\Theta = 10 \text{ mrad}$. In such case, the setup efficiency would be $\eta_{\text{setup}} \sim 0.9 \times 10^{-10}$.

In the EDM measurement, comparing to the MDM measurement, the deflection angle is more important than Lorentz factor and the number of deflected particles (see Eq. (26)). For this reason the optimal bending radius is smaller (see Fig. 8, right) and the optimal crystal length is greater. Dotted line in Fig. 8 (right) shows the EDM measurement efficiency when the crystal parameters are optimised for the MDM measurement. Optimising the setup for EDM measurement can gain a factor of two to the efficiency.

C. Preliminary study of the background from other decay channels

In the current study we consider the τ decay into three charged pions,

$$\tau^+ \rightarrow \pi^+\pi^+\pi^-\bar{\nu}_\tau. \quad (34)$$

The advantage of this decay channel is that the secondary vertex can be reconstructed and the final τ polarisation can be mainly reconstructed from the momenta of pions, which is also very important to maximise the value of S . We now consider possible processes producing $\pi^+\pi^+\pi^-$ secondary vertices at the end of the second crystal.

The double-crystal setup plays an important role for the background separation. Due to a small misalignment of the second crystal $\theta_v \sim 100 \mu\text{rad}$, the particle deflected by the first crystal cannot be involved into the channeling regime in the second one. This removes all charged D mesons decaying directly into $\pi^+\pi^+\pi^-$, as shown in Fig. 9. In addition, the planar channeling in a long crystal is possible only for positively charged particles. As a consequence, $\pi^+\pi^+\pi^-$ events can only come from the chain $pp \rightarrow X^+ \dots \rightarrow Y^+ \dots \rightarrow \pi^+\pi^+\pi^- \dots$.

To study the background from these decay channels, we used the Pythia 8.2 generator. Figure 9 shows the distribution over the invariant mass of the three reconstructed pions for the main decay channels, listed on the figures. The simulation shows that the main source of background is the decay $\tau^+ \rightarrow \pi^+\pi^+\pi^-\pi^0\bar{\nu}_\tau$. With a requirement on the invariant mass $\geq 1 \text{ GeV}$, we can reduce its contamination to 25%. For the present study, we suppose that the τ polarisation from the $\pi^+\pi^+\pi^-\pi^0$ decay channel is zero. This is a pessimistic assumption since the presence of π^0 should not completely break the correlation between the τ polarisation and the angular distribution of $\pi^+\pi^+\pi^-$. In addition, this background could be further reduced by the identification of the π^0

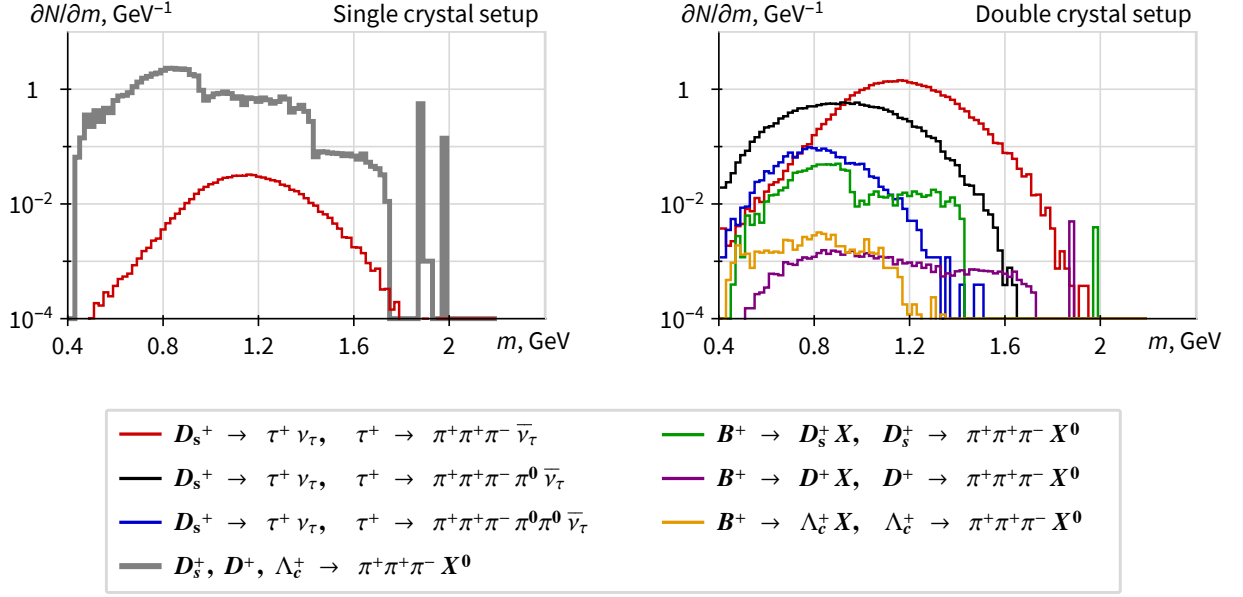


FIG. 9. Invariant mass distribution of $\pi^+\pi^+\pi^-$ combinations from (red line) the main decay chain, $D_s^+ \rightarrow \tau^+ \nu_\tau$, $\tau^+ \rightarrow \pi^+\pi^+\pi^- \bar{\nu}_\tau$, and for the background decay chains with $\pi^+\pi^+\pi^-$ in the final state and listed at the bottom, using (left) a single-crystal setup and (right) a double-crystal setup.

meson. Other sources of background come from B -meson decays, but as shown in Fig. 9, they are negligible. A detailed study could be performed to evaluate the background coming from accidental reconstruction of three pion vertices.

D. Results of the sensitivity studies

In this section, we study the efficiency of the double-crystal setup proposed in the previous section and determine the optimal parameters of the setup for a 7 TeV proton beam. They are:

- Target: tungsten with $L_{\text{tar}} = 1$ cm;
- Crystal 1: germanium with $L_D = 3$ cm, $R_D = 10$ m and $\theta_p = 100 \mu\text{rad}$;
- Crystal 2: germanium with $L = 10$ cm, $R = 7$ m and $\theta_v = 80 \mu\text{rad}$, at $L_v = 10$ cm.

In this study, we did not look in details at the detection system. We consider the analysis of the decay channel $\tau^+ \rightarrow \pi^+\pi^+\pi^- \bar{\nu}_\tau$ ($Br = 0.0899$ [1]) and suppose a detection efficiency of $\eta_{\text{det}} = 50\%$. In Table II we present (column 3) the efficiencies of each process, starting from D_s^+ production in the target, up to reconstruction of MDM and EDM of τ lepton, and (column 4) the total efficiencies,

TABLE II. Efficiency of the measurement: current (by process) and total (per incident proton).

| Place | process (factors) | double crystal setup | | single crystal setup | |
|-----------|---|--------------------------|---------------------------|--------------------------|---------------------------|
| | | current | total | current | total |
| target | $p \rightarrow D_s^+, D_s^+$ decay | $1.1 \cdot 10^{-4}$ | $1.1 \cdot 10^{-4}$ | $1.1 \cdot 10^{-4}$ | $1.1 \cdot 10^{-4}$ |
| crystal 1 | D_s^+ collimation | $0.8 \cdot 10^{-2}$ | $0.9 \cdot 10^{-6}$ | — | — |
| crystal 1 | D_s^+ deflection | $1.3 \cdot 10^{-1}$ | $1.1 \cdot 10^{-7}$ | — | — |
| void | $D_s^+ \rightarrow \tau^+$ | $1.2 \cdot 10^{-2}$ | $1.4 \cdot 10^{-9}$ | $0.5 \cdot 10^{-3}$ | $0.5 \cdot 10^{-7}$ |
| crystal 2 | τ^+ collimation | $0.5 \cdot 10^{-1}$ | $0.7 \cdot 10^{-10}$ | $1.7 \cdot 10^{-2}$ | $0.9 \cdot 10^{-9}$ |
| crystal 2 | τ^+ deflection | $0.3 \cdot 10^{-1}$ | $2.2 \cdot 10^{-12}$ | $0.3 \cdot 10^{-1}$ | $0.3 \cdot 10^{-12}$ |
| detector | $\eta_{\text{det}} \times Br$ | $0.4 \cdot 10^{-1}$ | $1.0 \cdot 10^{-13}$ | $0.4 \cdot 10^{-1}$ | $1.3 \cdot 10^{-12}$ |
| reconstr. | $\eta_{\text{MDM}} \sim \langle \mathbb{P}^2 \gamma^2 \rangle \theta^2 S^2$ | ~ 8 | $\sim 0.7 \cdot 10^{-12}$ | ~ 0.5 | $\sim 0.7 \cdot 10^{-12}$ |
| reconstr. | $\eta_{\text{EDM}} \sim \langle \mathbb{P}^2 \gamma^2 \rangle \theta^4 S^2$ | $\sim 1.5 \cdot 10^{-3}$ | $\sim 1.5 \cdot 10^{-16}$ | $\sim 1.1 \cdot 10^{-4}$ | $\sim 1.5 \cdot 10^{-16}$ |

i.e. the number of D_s^+ or τ after each stage of double crystal setup referred to the total number of impinging protons on target. Last two rows in the table present efficiencies of MDM and EDM reconstruction. Using latter, we can rewrite Eqs. (24) and (27) in a following way

$$\Delta a_\tau = \frac{1}{\sqrt{N_{\text{POT}} \eta_{\text{MDM}}}} \quad \Delta d_\tau = \frac{\mu_B}{2 \sqrt{N_{\text{POT}} \eta_{\text{EDM}}}} \quad (35)$$

where Δd_τ is the absolute statistical error of the measured EDM in units [e cm] and μ_B is the Bohr magneton.

We also estimate the efficiency of the single crystal setup presented in Fig. 3 (see columns 5 and 6 in Table II). The numbers in the table correspond to the following properties of the single crystal setup: germanium crystal with $L = 10$ cm, $R = 7$ m and $\theta_p = 100 \mu\text{rad}$ at $L_v = 40$ cm, from 1 cm tungsten target. We found that in order to reach the reconstruction efficiency of double crystal setup the conversion length should not be greater than $L_v = 40$ cm. On the other hand, such length is too short to reconstruct the $D_s^+ \rightarrow \tau^+ \nu_\tau$ vertex, i.e. to verify that the signal comes from the τ lepton produced before the crystal, but not inside or after the one, or from other particle with a similar final state (see Fig. 9). Due to these reasons we consider the double crystal setup to be more efficient. Note, that due to a greater average polarisation, the double crystal setup has a better reconstruction efficiency of MDM and EDM (referred to one deflected τ lepton).

Figure 10 (left) shows the absolute statistical error of the measured anomalous MDM of the τ lepton using Eq. (24) as a function of the total number of protons on target. The blue lines show the sensitivity of the present analysis by varying in particular the value of S in the range

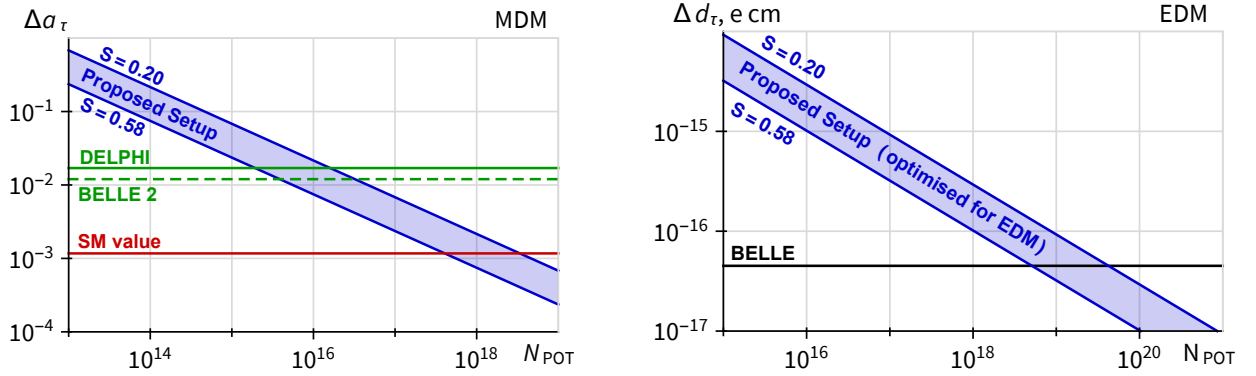


FIG. 10. Absolute statistical error (left) of the anomalous MDM, (right) of EDM of the τ lepton.

$0.2 < S < 0.58$. The maximal value corresponds to the limit on the accuracy, in case all observables are fully reconstructed. The green lines show the limits obtained by the DELPHI collaboration [7] and expected for the BELLE 2 experiment [23]. The red line represents the value of the τ anomalous MDM predicted by the SM [6]. Further detailed studies will be performed to improve the current efficiency. In particular, detailed background studies could allow us to use one prong τ decays.

For EDM measurement this setup is not very efficient. Even when optimised for EDM measurement, the current experimental accuracy on EDM [13] could be achieved only after about 10^{19} POT, which is probably not realistic (see Fig. 10 (right)).

IV. CONCLUSIONS

In this paper, we propose a method of a direct measurement of the anomalous magnetic dipole moment (MDM) of the τ lepton by studying its spin precession using a double-crystal setup at the LHC. Our study shows that with this proposal, one can reach the present accuracy on the τ MDM using 10^{16} protons on target. A total of 10^{18} protons on target are needed to reach an accuracy equivalent to the Standard Model value. The measurement of EDM is even more challenging and a further order of magnitude of POT is needed to reach the present experimental accuracy. The benefit of this method is that there is no assumption on the value of the τ electric dipole moment. This study opens up the possibility of doing a single dedicated experiment to measure both the MDM of charmed baryons [27–32] and of τ lepton at the LHC.

Appendix A: Polarisation of τ leptons in D_s decays

We consider the decay of the D_s meson

$$D_s^+(p) \rightarrow \tau^+(k) + \nu_\tau(q), \quad (\text{A1})$$

with $p = k + q$, and find the polarisation vector of the τ lepton. The four-momentum of the D_s meson is $p^\mu = (E_D, \vec{p}_D)$. We further assume that the neutrino is massless.

To describe the polarisation of a fermion in its rest frame, one introduces the vector $\vec{\xi}$ ($|\vec{\xi}| \leq 1$). In the frame in which fermion moves with the four-momentum $k^\mu = (\varepsilon_\tau, \vec{k}_\tau)$, the polarisation four-vector is [41]

$$a^\mu = \left(\frac{\vec{k}_\tau \cdot \vec{\xi}}{m_\tau}, \vec{\xi} + \frac{\vec{k}_\tau (\vec{k}_\tau \cdot \vec{\xi})}{m_\tau(m_\tau + \varepsilon_\tau)} \right), \quad (\text{A2})$$

with the conditions $k \cdot a = 0$ and $a^2 = -\xi^2$.

We can write matrix element of the D_s^+ decay as

$$\mathcal{M} = \frac{g^2}{8M_W^2} f_D V_{cs}^* p^\mu \bar{u}(q) \gamma_\mu (1 - \gamma_5) v(k), \quad (\text{A3})$$

where f_D is the weak-decay constant of the $D_s^+ \rightarrow \tau^+ \nu_\tau$ decay, M_W is the mass of the W boson, V_{cs} is the element of the Cabibbo-Kobayashi-Maskawa matrix, $g = e/\sin\theta_W$, e is the positron charge and θ_W is the weak mixing angle.

Using the spin-density matrix of the τ^+ lepton,

$$v(k) \bar{v}(k) = \frac{1}{2} (\not{k} - m_\tau) (1 + \gamma_5 \not{\phi}), \quad (\text{A4})$$

one obtains the probability to find the τ^+ lepton with polarisation a^μ . It is proportional to

$$|\mathcal{M}|^2 = \frac{g^4 m_\tau^2}{16M_W^4} |V_{cs}|^2 f_D^2 (k \cdot q - m_\tau p \cdot a), \quad (\text{A5})$$

with $k \cdot q = (M_D^2 - m_\tau^2)/2$.

Equation (A5) allows one to find the τ polarisation vector $\vec{\mathbb{P}}$ which arises in the decay process. For this we write

$$(k \cdot q - m_\tau p \cdot a) \equiv k \cdot q \left(1 + \vec{\xi} \cdot \vec{\mathbb{P}} \right), \quad (\text{A6})$$

$$\vec{\mathbb{P}} = \frac{1}{k \cdot q} \left[m_\tau \vec{p}_D - E_D \vec{k}_\tau + \frac{\vec{k}_\tau (\vec{k}_\tau \cdot \vec{p}_D)}{m_\tau + \varepsilon_\tau} \right]. \quad (\text{A7})$$

The corresponding polarisation four-vector in an arbitrary frame has a form similar to Eq. (A2), namely

$$S^\mu = \left(\frac{\vec{k}_\tau \cdot \vec{\mathbb{P}}}{m_\tau}, \vec{\mathbb{P}} + \frac{\vec{k}_\tau (\vec{k}_\tau \cdot \vec{\mathbb{P}})}{m_\tau (m_\tau + \varepsilon_\tau)} \right), \quad (\text{A8})$$

where $k \cdot S = 0$ and $S^2 = -\vec{\mathbb{P}}^2$. One can also write S^μ explicitly in terms of the four-momenta of the D_s meson and the τ lepton, using Eqs. (A7) and (A8),

$$S^\mu = \frac{m_\tau}{k \cdot q} \left(p^\mu - k^\mu \frac{k \cdot p}{m_\tau^2} \right), \quad (\text{A9})$$

where $S^2 = -1$. It follows that $\vec{\mathbb{P}}^2 = 1$, so that the τ lepton is 100 % polarised.

Appendix B: Optimal length for D_s conversion to τ leptons

We consider τ leptons produced in the decay of D_s mesons and the consequent τ decay. Thus, there are two competing processes, production and decay of the τ lepton.

The probability of τ production in the process $D_s^+ \rightarrow \tau^+ \nu_\tau$ at the D_s flight length x is

$$N_{\text{prod}} = \mathcal{B}_i \left(1 - e^{-x/T_D} \right), \quad (\text{B1})$$

where $\mathcal{B}_i = \Gamma_i/\Gamma \approx 0.055$ [1] is the branching ratio of the current process, $T_D = c \tau_D \gamma_D$ is the decay length of a boosted D_s meson ($c \tau_D \approx 150 \mu\text{m}$). The probability of τ decay after a flight length of $L_v - x$ is

$$N_{\text{dec}} = e^{-(L_v - x)/T_\tau}, \quad (\text{B2})$$

where $T_\tau = c \tau_\tau \gamma_\tau$ is the decay length of a boosted τ lepton ($c \tau_\tau \approx 87 \mu\text{m}$).

The conversion efficiency, that is the ratio of the number of τ leptons not decayed after the flight length L_v , to the initial number of D_s mesons of energy E_D is

$$\eta(L_v, E_D) = \frac{\int_{\varepsilon_\tau^{\min}}^{\varepsilon_\tau^{\max}} d\varepsilon_\tau \frac{\partial N_\tau}{\partial \varepsilon_\tau} \int_0^{L_v} dx \frac{\partial N_{\text{prod}}}{\partial x} N_{\text{dec}}(L_v - x)}{\int_{\varepsilon_\tau^{\min}}^{\varepsilon_\tau^{\max}} d\varepsilon_\tau \frac{\partial N_\tau}{\partial \varepsilon_\tau}}, \quad (\text{B3})$$

where $\partial N_\tau / \partial \varepsilon_\tau$ is the τ spectrum. In a two-body decay, the τ spectrum is defined by the energy of the D_s meson, but in our experimental setup, τ leptons are later captured into a channeling regime, and hence are collimated in angle and energy in a quite complicated way (see Fig. 6,7). Thus, in this case it is useful to find the extreme values of the conversion efficiency $\eta(L_v, E_D)$ that correspond to the extreme values of the τ energy.

The energy range of τ leptons produced in a two-body decay of D_s mesons in the relativistic case is

$$\varepsilon_\tau \in E_D \left[\frac{m_\tau^2}{M_D^2}, 1 \right]. \quad (\text{B4})$$

Substituting Eqs. (B1) and (B2) into Eq. (B3) and considering a mono-energetic τ spectrum of energy ε_τ^* , we obtain

$$\eta^*(L_v, E_D, \varepsilon_\tau^*) = Br_i \frac{e^{-L_v/T_D} - e^{-L_v/T_\tau}}{T_D/T_\tau - 1}. \quad (\text{B5})$$

Figure 11 presents the conversion efficiency as a function of the path length for three D_s energies, listed in the figure. The width of the curves represents energy spread of the τ lepton. The upper and lower edges correspond to upper and lower limits of the τ energy given in Eq. (B4).

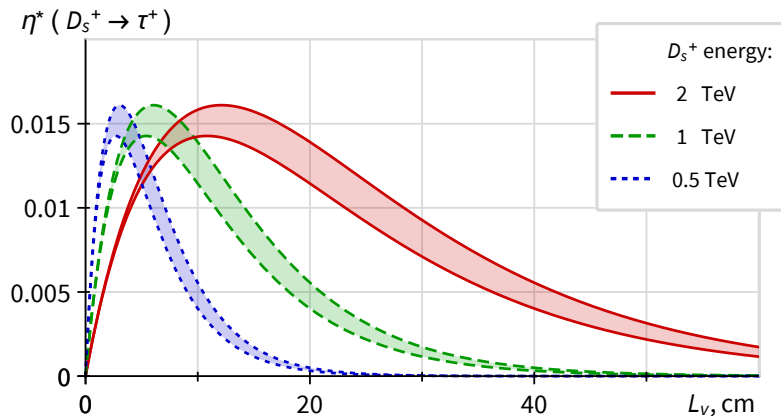


FIG. 11. $D_s^+ \rightarrow \tau^+$ conversion efficiency as a function of the flight length.

The optimal length for the D_s conversion to τ leptons strongly depends on the D_s spectrum. For the energy range $1 \text{ TeV} < E_D < 2 \text{ TeV}$, the optimal length is around 10 cm. Considering conversion lengths $L_v > 40 \text{ cm}$ would essentially reduce the part of the spectra to $E_D < 2 \text{ TeV}$.

ACKNOWLEDGMENTS

This research was partially conducted in the scope of the IDEATE International Associated Laboratory (LIA). A.Yu.K. and A.S.F. acknowledge partial support by the National Academy of Sciences of Ukraine (project KPKVK 6541230, and project no. Ts-3/53-2018) and the Ministry of Education and Science of Ukraine (project no. 0117U004866).

-
- [1] M. Tanabashi et al. Review of Particle Physics. *Phys. Rev.*, D98(3):030001, 2018.
 - [2] G.W. Bennett et al. Final report of the Muon E821 anomalous magnetic moment measurement at BNL. *Phys. Rev.*, D73:072003, 2006.
 - [3] M. Knecht. The Anomalous magnetic moment of the muon: A Theoretical introduction. *Lect. Notes Phys.*, 629:37, 2004.
 - [4] M. Passera. The Standard model prediction of the muon anomalous magnetic moment. *J. Phys. G.*, 31(R75), 2005.
 - [5] F. Jegerlehner and A. Nyffeler. The Muon $g-2$. *Phys. Rept.*, 477:1–110, 2009.
 - [6] S. Eidelman and M. Passera. Theory of the tau lepton anomalous magnetic moment. *Mod. Phys. Lett.*, A22:159–179, 2007.
 - [7] J. Abdallah et al. Study of tau-pair production in photon-photon collisions at LEP and limits on the anomalous electromagnetic moments of the tau lepton. *Eur. Phys. J.*, C35:159–170, 2004.
 - [8] F. Cornet and J. I. Illana. Tau pair production via photon-photon collisions at LEP. *Phys. Rev.*, D53:1181–1184, 1996.
 - [9] G. A. Gonzalez-Sprinberg, A. Santamaria, and J. Vidal. Model independent bounds on the tau lepton electromagnetic and weak magnetic moments. *Nucl. Phys.*, B582:3–18, 2000.
 - [10] B. L. Roberts and W. J. Marciano. Lepton dipole moments. *Adv. Ser. Direct. High Energy Phys.*, 20: 1–757, 2009.
 - [11] E. D. Commins. Electric dipole moments of leptons. *Adv. At. Mol. Opt. Phys.*, 40:1-55, 1999.
 - [12] E. D. Commins and D. DeMille. The electric dipole moment of the electron. *Adv. Ser. Direct. High Energy Phys.*, 20: 519–581, 2009.
 - [13] K. Inami *et al.* [Belle Collaboration]. Search for the electric dipole moment of the tau lepton. *Phys. Lett.*, B551:16–26, 2003.
 - [14] A. Hayreter and G. Valencia. Constraints on anomalous color dipole operators from Higgs boson production at the LHC. *Phys. Rev.*, D88:034033, 2013.
 - [15] A. Hayreter and G. Valencia. Spin correlations and new physics in τ -lepton decays at the LHC. *JHEP*, 07:174, 2015.

- [16] S. Atag and A. A. Billur. Possibility of determining τ lepton electromagnetic moments in $\gamma\gamma \rightarrow \tau^+\tau^-$ process at the CERN-LHC. *JHEP*, 11:060, 2010.
- [17] M. Köksal, S. C. İnan, A. A. Billur, Y. Ozguven and M. K. Bahar. Analysis of the anomalous electromagnetic moments of the tau lepton in γp collisions at the LHC. *Phys. Lett.*, B783:375–380, 2018.
- [18] M. Köksal, A. A. Billur, A. Gutiérrez-Rodríguez and M. A. Hernández-Ruíz. Model-independent sensitivity estimates for the electromagnetic dipole moments of the τ -lepton at the CLIC. *Phys. Rev.*, D98:015017, 2018.
- [19] Y. Ozguven, S. C. İnan, A. A. Billur, M. Köksal and M. K. Bahar. Search for the anomalous electromagnetic moments of tau lepton through electronphoton scattering at CLIC. *Nucl. Phys.*, B923:475–490, 2017.
- [20] M. Köksal. Search for the electromagnetic moments of the τ lepton in photon-photon collisions at the LHeC and the FCC-he. arXiv:1809.01963 [hep-ph].
- [21] J. Bernabeu, G. A. Gonzalez-Sprinberg, J. Papavassiliou, et al. Tau anomalous magnetic moment form-factor at super B/charm factories. *Nucl. Phys.*, B790:160–174, 2008.
- [22] J. Bernabeu, G. A. Gonzalez-Sprinberg, and J. Vidal. Tau spin correlations and the anomalous magnetic moment. *JHEP*, 01:062, 2009.
- [23] S. Eidelman, D. Epifanov, M. Fael, et al. τ dipole moments via radiative leptonic τ decays. *JHEP*, 03:140, 2016.
- [24] M. Fael and M. Passera. Precision tests via radiative μ and τ leptonic decays. *PoS*, RADCOR2015:091, 2016.
- [25] M. A. Samuel, G. Li, and R. Mendel. The Anomalous magnetic moment of the tau lepton. *Phys. Rev. Lett.*, 67:668–670, 1991. [Erratum: *Phys. Rev. Lett.* 69,995(1992)].
- [26] D. Chen et al. First observation of magnetic moment precession of channeled particles in bent crystals. *Phys. Rev. Lett.*, 69:3286–3289, 1992.
- [27] V.G. Baryshevsky. The possibility to measure the magnetic moments of short-lived particles (charm and beauty baryons) at LHC and FCC energies using the phenomenon of spin rotation in crystals. *Phys. Lett.*, B757:426–429, 2016.
- [28] A. S. Fomin et al. Feasibility of measuring the magnetic dipole moments of the charm baryons at the LHC using bent crystals. *JHEP*, 08:120, 2017.
- [29] F.J. Botella, L.M. Garcia Martin, D. Marangotto, et al. On the search for the electric dipole moment of strange and charm baryons at LHC. *Eur. Phys. J.*, C77(3):181, 2017.
- [30] E. Bagli et al. Electromagnetic dipole moments of charged baryons with bent crystals at the LHC. *Eur. Phys. J.*, C77(12):828, 2017.
- [31] V. G. Baryshevsky. Spin rotation and depolarization of high-energy particles in crystals at LHC and FCC energies. The possibility to measure the anomalous magnetic moments of short-lived particles and quadrupole moment of Λ -hyperon. *Nucl. Instrum. Meth.*, B402:5–10, 2017.

- [32] A. Fomin. *Multiple scattering effects on the dynamics and radiation of fast charged particles in crystals. Transients in the nuclear burning wave reactor*. PhD thesis, Paris-Sud University: PHENIICS, Orsay, France, September 2017.
- [33] M. Davier, L. Duflot, F. Le Diberder, et al. The Optimal method for the measurement of tau polarization. *Phys. Lett.*, B306:411–417, 1993.
- [34] K. Hagiwara, A. D. Martin, and D. Zeppenfeld. Tau Polarization Measurements at LEP and SLC. *Phys. Lett.*, B235:198–202, 1990.
- [35] A. Rouge. Polarization observables in the 3 pi neutrino decay mode. *Z. Phys.*, C48:75–78, 1990.
- [36] L. Duflot. *Nouvelle méthode de mesure de la polarisation du τ . Application au canal $\tau \rightarrow a_1 \nu_\tau$ dans l'expérience ALEPH*. PhD thesis, Orsay, LAL, 1993.
- [37] V.G. Baryshevsky. Spin rotation of ultrarelativistic particles passing through a crystal. *Sov. Tech. Phys. Lett.*, 5:73, 1979. [*Pis'ma. Zh. Tekh. Fiz.* 5 (1979) 182].
- [38] V.L. Lyuboshits. The spin rotation at deflection of relativistic charged particle in electric field. *Sov. J. Nucl. Phys.*, 31:509, 1980. [*Yad. Fiz.*31,986(1980)].
- [39] I.J. Kim. Magnetic moment measurement of baryons with heavy flavored quarks by planar channeling through bent crystal. *Nucl. Phys.*, B229:251–268, 1983.
- [40] T. Sjostrand, S. Mrenna, and P. Z. Skands. A Brief Introduction to PYTHIA 8.1. *Comput. Phys. Commun.*, 178:852–867, 2008.
- [41] V. B. Beresteckii, E. M. Lifshitz, and L. P. Pitaevskii. *Quantum electrodynamics*. Pergamon Press, 1982.